Human Molecular Genetics, 2006, Vol. 15, No. 8 ***1343–1353***
doi:10.1093/hmg/ddl054
Advance Access published on March 14, 2006

SPG3A protein atlastin-1 is enriched in growth cones and promotes axon elongation during neuronal development

Peng-Peng Zhu[1], Cynthia Soderblom[1], Jung-Hwa Tao-Cheng[2], Julia Stadler[1] and Craig Blackstone[1,*]

[1]Cellular Neurology Unit and [2]Electron Microscopy Facility, National Institute of Neurological Disorders and Stroke, National Institutes of Health, Bethesda, MD 20892, USA

Received January 12, 2006; Revised and Accepted March 7, 2006

The hereditary spastic paraplegias (HSPs) (SPG1-29) comprise a group of inherited neurological disorders characterized principally by spastic lower extremity weakness due to a length-dependent, retrograde axonopathy of corticospinal motor neurons. Mutations in the gene encoding the dynamin superfamily member atlastin-1, an oligomeric GTPase highly localized to the Golgi apparatus in the adult brain, are responsible for SPG3A, a common autosomal dominant HSP. A distinguishing feature of SPG3A is its frequent early onset, raising the possibility that developmental abnormalities may be involved in its pathogenesis. Here, we demonstrate that several missense SPG3A mutant atlastin-1 proteins have impaired GTPase activity and thus may act in a dominant-negative, loss-of-function manner by forming mixed oligomers with wild-type atlastin-1. Using confocal and electron microscopies, we have also found that atlastin-1 is highly enriched in vesicular structures within axonal growth cones and varicosities as well as at axonal branch points in cultured cerebral cortical neurons, prefiguring a functional role for atlastin-1 in axonal development. Indeed, knockdown of atlastin-1 expression in these neurons using small hairpin RNAs reduces the number of neuronal processes and impairs axon formation and elongation during development. Thus, the 'long axonopathy' in early-onset SPG3A may result from abnormal development of axons because of loss of atlastin-1 function.

INTRODUCTION

The hereditary spastic paraplegias (HSPs) constitute a clinically and genetically diverse cluster of inherited neurological disorders in which the primary manifestations are progressive spasticity and weakness of the lower limbs due to a length-dependent, retrograde axonopathy of the upper motor neurons in the cerebral cortex (1–4). These disorders have historically been classified as 'pure' if spastic paraplegia occurs in isolation or 'complicated' if other neurological abnormalities are present (5). Concordant with their clinical presentation, several neuropathological studies of the HSPs have revealed distal axonal degeneration in the long descending corticospinal tracts as well as the long ascending dorsal column fibers in the spinal cord, the latter constituting some of the longest sensory axons in the nervous system. This axonal degeneration is length dependent and largely spares the neuronal cell soma. Interestingly, thinning of the corticospinal tracts has been reported in some patients with early-onset HSP, suggesting that abnormal development may be involved in some forms of HSP (4).

The identification over the past several years of >25 genetic loci and 11 gene products for the HSPs has yielded new insights into their pathogenesis (1–4). Indeed, causative mutations have been identified in proteins within several broad functional categories: mitochondrial function, axonal development, intracellular trafficking and transport and myelination. Among these categories, the largest number of identified gene products appears generally related to protein or membrane trafficking, although, in many cases, direct evidence is lacking (1–4).

The autosomal dominant HSP SPG3A is the second most common HSP and is caused by more than 20 different mutations, predominantly missense mutations, in the *atlastin-1*

*To whom correspondence should be addressed at: Cellular Neurology Unit, NINDS, National Institutes of Health, Building 35, Room 2C-913, 35 Convent Drive, Bethesda, MD 20892-3704, USA. Tel: +1 3014519680; Fax: +1 3014804888; Email: blackstc@ninds.nih.gov

Published by Oxford University Press 2006.

Downloaded from https://academic.oup.com/hmg/article/15/8/1343/644573 by guest on 23 April 2024

gene (6,7) (Supplementary Material, Fig. S1). On the basis of some sequence similarity to proteins in the dynamin superfamily of large GTPases (6,8), atlastin-1 has been implicated in intracellular membrane trafficking. However, although the atlastin-1 GTPase is known to be an oligomeric GTPase highly localized to the Golgi apparatus in the adult brain (9), the effects of SPG3A mutations on atlastin-1 structure and activity are not known, nor are their effects on neuronal function within the central nervous system. Here, we report that several common atlastin-1 mutations impair atlastin-1 GTPase activity. Furthermore, in addition to its localization to the Golgi apparatus, atlastin-1 is also highly enriched in axonal growth cones and varicosities during central nervous system development, and loss of atlastin-1 inhibits the growth of axons. These findings are consistent with a neurodevelopmental etiology for the very early-onset SPG3A form of HSP.

RESULTS

SPG3A mutations impair atlastin-1 GTPase activity but not oligomerization

To understand better the molecular pathogenesis of autosomal dominant SPG3A, we investigated several different known SPG3A missense mutations for their effects on atlastin-1 homo-oligomerization and GTPase activity (9). Using yeast two-hybrid assays, we found that several different SPG3A mutant forms interacted robustly with wild-type atlastin-1 (Fig. 1A). Next, we evaluated the interactions between SPG3A and wild-type atlastin-1 proteins over-expressed in COS-7 cells. By immunoblot analysis, these proteins were expressed at similar levels (Fig. 1B), and they were similarly localized to the membrane fraction (Fig. 1C). Co-immunoprecipitation (IP) studies with differentially tagged mutant and wild-type atlastin-1 proteins confirmed that the mutant and wild-type proteins are able to associate in cells (Fig. 1D). Using FPLC gel-exclusion chromatography, we found that detergent-solubilized wild-type and all SPG3A mutant forms of atlastin-1 examined eluted as presumptive oligomers in a single peak (Fig. 1E). Interestingly, Myc-tagged wild-type atlastin-1 and SPG3A atlastin-1 H258R eluted at similar native sizes of 283 ± 16 kDa ($n = 5$) and 297 ± 24 kDa ($n = 5$), respectively, whereas the SPG3A mutant forms R217Q (222 ± 5 kDa; $n = 4$) and R239C (210 ± 10 kDa; $n = 5$) eluted at slightly smaller calculated sizes. To determine whether these differences reflected changes in oligomerization state or conformation, we performed chemical cross-linking studies using the homobifunctional, amino-reactive cross-linker *bis*(sulfosuccinimidyl)suberate (BS^3), followed by denaturing SDS–PAGE. We found that the cross-linking results for wild-type and SPG3A atlastin-1 proteins were remarkably similar (Fig. 1F). Thus, it appears most likely that the wild-type and SPG3A atlastin-1 proteins oligomerize to the same extent but that conformation changes in some SPG3A mutant forms may influence the apparent sizes of the detergent-solubilized oligomers in FPLC gel-exclusion chromatography studies.

We considered the possibility that SPG3A mutations might affect atlastin-1 GTPase activity and, subsequently, that these mutant atlastin-1 proteins might functionally impair the atlastin-1 oligomer by binding to wild-type atlastin-1 proteins and reducing overall complex GTPase activity in a dominant-negative manner. In one identified SPG3A missense mutation, R217Q, the involved residue is within the highly conserved tripartite GTP binding site (10), and in fact, an affinity-purified calmodulin-binding protein (CBP)–atlastin-1 R217Q fusion protein showed a dramatic reduction in GTPase activity when compared with the wild-type CBP–atlastin-1 fusion protein (Fig. 2). Other SPG3A missense mutants involving nearby residues not within the highly conserved GTP tripartite binding motifs also exhibited decreased GTPase activity (Fig. 2), suggesting that these regions may be modulatory. Thus, although these studies examined oligomers composed entirely of mutant proteins, it seems likely that binding of mutant atlastin-1 molecules with impaired GTPase activity to wild-type molecules would decrease overall atlastin-1 complex GTPase activity.

Atlastin-1 is enriched in axonal growth cones during development

Abnormalities in central nervous system development have been proposed for SPG3A because of its often very early onset as well as its slow progression and, in some cases, lack of apparent progression (2,6,7,11–15); thus, we looked for changes in the developmental expression of the atlastin-1 protein. Interestingly, by immunoblot analysis of rat brain homogenates, atlastin-1 levels increased gradually from embryonic day 18 (E18) through adulthood, but much less so than synaptic markers such as synaptophysin, whereas levels of Golgi apparatus markers such as p115 and endoplasmic reticulum (ER) markers such as calnexin were essentially unchanged (Fig. 3). Upon fractionation of homogenized rat cortical neurons by sucrose gradient density centrifugation, we observed only partial overlap of fractions enriched in Golgi (p115) and ER (Grp78) markers with those enriched in atlastin-1 (Fig. 4). Taken together, these results indicate that atlastin-1 may be localized to other cellular structures in addition to the Golgi apparatus and ER during neuronal development.

We examined the localization of atlastin-1 in developing rat cortical neurons in primary culture using confocal immunofluorescence microscopy (Fig. 5). Interestingly, atlastin-1 was highly enriched not only in Golgi apparatus but also in axonal growth cones and growth cone-like varicosities, or 'waves' (16,17), distributed along the axons and at branch points (Fig. 5A). Markers for the Golgi apparatus, however, were not found in these growth cones or varicosities (Fig. 5A). Partial co-localization was seen with atlastin-1 and markers of the ER in the cell soma, but ER markers were not present within axonal varicosities or growth cones (Fig. 5B). Importantly, although the majority of growth cones were stained with atlastin-1 antibodies, some growth cones were unstained (data not shown). No co-localization of atlastin-1 with synaptic markers such as synaptophysin was found, indicating that atlastin-1 is not present at synapses (data not shown).

We investigated the localization of atlastin-1 in growth cones and varicosities in more detail using co-localization

Downloaded from https://academic.oup.com/hmg/article/15/8/1343/644573 by guest on 23 April 2024

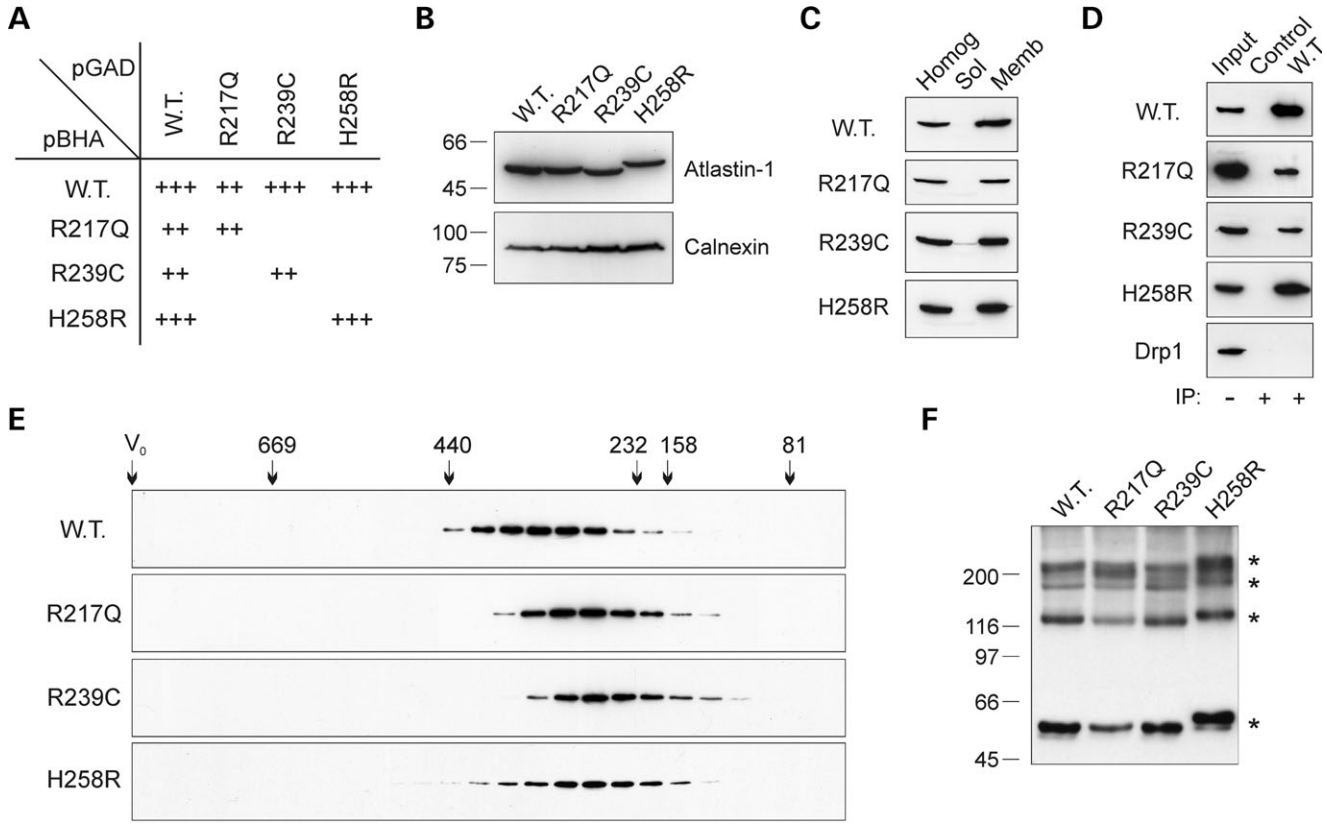

Figure 1. Effects of SPG3A mutations on atlastin-1 oligomerization. (**A**) Matrix of yeast two-hybrid interactions for the indicated wild-type and SPG3A mutant atlastin-1 bait (pBHA) and prey (pGAD constructs). Strength of interaction was assayed by *HIS3* and β-*galactosidase* induction. β-Galactosidase activity was assessed by determining the time for colonies to turn blue in an X-gal filter lift assay: +++, <30 min; ++, 30–60 min; +, 60–120 min; −, no significant activity. HIS3 activity was quantified by determining the percentage of colonies growing on histidine-lacking when compared with histidine-containing media: +++, >75%; ++, 50–75%; +, <50%; −, no significant growth. In all cases, *HIS3* and β-*galactosidase* induction correlated. None of the bait constructs used exhibited self-activation in control experiments. (**B**) Expression of the indicated Myc-tagged wild-type (WT) and SPG3A mutant atlastin-1 proteins in COS-7 cells (20 μg protein/lane), with immunodetection using anti-Myc antibodies. The ER protein calnexin was used as a loading control. Migrations of molecular mass standards (in kDa) are shown on the left. (**C**) Membrane association of Myc-tagged wild-type and SPG3A mutant atlastin-1 proteins over-expressed in COS-7 cells. In all cases, the atlastin-1 proteins fractionated in the lysed membrane pellet (Memb), but not the soluble cytosolic fraction (Sol) derived from ultracentrifugation of the post-nuclear supernatant, with detection using anti-Myc antibodies. 'Homog' represents the total cell homogenate. (**D**) Co-IP of SPG3A mutant and wild-type atlastin-1 proteins. HA-tagged wild-type atlastin-1 (WT) was co-expressed with the indicated Myc-tagged SPG3A mutant atlastin-1 proteins or else the Myc-tagged Drp1 mitochondrial dynamin-like GTPase (which does not interact with atlastin-1) as a control, and the cell extracts were IP with anti-HA antibodies. Precipitates were then immunoblotted with anti-Myc antibodies. 'Input' represents 20% of the starting material. To further confirm specificity of the IPs, extracts from cells expressing Myc-tagged atlastin-1 or Myc-Drp1 proteins alone were IP with anti-HA antibodies (Control). (**E**) Detergent-solubilized extracts prepared from cells over-expressing Myc-tagged wild-type (WT) or SPG3A mutant forms of atlastin-1 were subjected to FPLC gel-exclusion chromatography, and aliquots of each collected fraction were immunoblotted with anti-Myc antibodies. The void volume (V_0) and elution peaks for marker proteins (in kDa) are indicated across the top. (**F**) Chemical cross-linking. Extracts from COS-7 cells over-expressing either wild-type (WT) or SPG3A mutant atlastin-1 proteins were subjected to chemical cross-linking with BS^3 and immunoblotted with anti-Myc antibodies. Asterisks denote the major cross-linked products on the right. Migrations of molecular mass standards (in kDa) are shown on the left.

studies with proteins such as GAP-43, which is known to be present in axonal varicosities as well as in growth cones (16). Axonal growth cones are organized into central (C) and peripheral (P) domains and, interestingly, atlastin-1 distribution in growth cones of cultured neurons occurred in two strikingly distinct patterns. In many cases, atlastin-1 appeared concentrated in the C-domain (Fig. 6A, upper panel), whereas in other cases, it appeared more peripherally at the leading edge of the growth cone in the P-domain (lower panel); a small number of atlastin-1 immunoreactive puncta were also found within the filopodia, sometimes at their distal tips (Fig. 6A). Although GAP-43 is also highly enriched in growth cones, co-localization with atlastin-1 at the subcellular level within the growth cones appeared limited (Fig. 6A). The microtubule-associated protein tau-1 is abundant in growth cones and varicosities, although, in contrast to atlastin-1, it is also diffusely present throughout the axon (Fig. 6B). Clathrin is another protein enriched within axonal growth cones and varicosities, and it co-localized prominently with atlastin-1 in a number of varicosities (Fig. 6C). In contrast, there was only partial co-localization of clathrin with atlastin-1 in the Golgi apparatus (Fig. 6C, lower panel). Lastly, the AP-2 adaptor complex, which binds clathrin and a number of other vesicle trafficking proteins, also co-localized with atlastin-1 prominently in axonal growth cones and growth cone-like varicosities, whereas there was

Downloaded from https://academic.oup.com/hmg/article/15/8/1343/644573 by guest on 23 April 2024

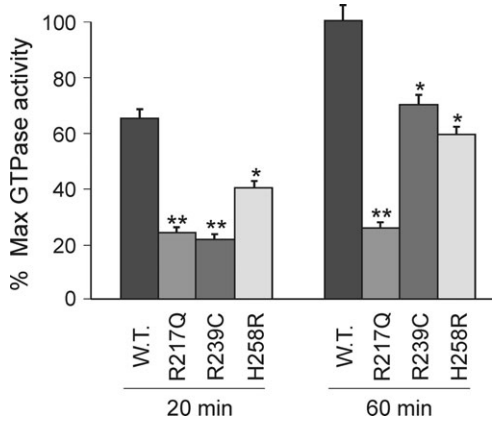

Figure 2. Effects of SPG3A mutations on atlastin-1 GTPase activity. Purified CBP-1 fusion proteins for wild-type atlastin-1 and the indicated SPG3A atlastin-1 mutants were incubated with [α-^{32}P]GTP for 20 or 60 min. [^{32}P]GDP and [^{32}P]GTP were resolved by separation on thin layer chromatography plates and quantified, and the percentage of hydrolysis calculated as described previously (9). Activity (expressed as a percentage of maximum GTPase activity for wild-type atlastin-1 at 60 min) at the indicated time points is depicted graphically. Values represent mean ± SD of at least three trials. $^{*}P < 0.05$; $^{**}P < 0.01$.

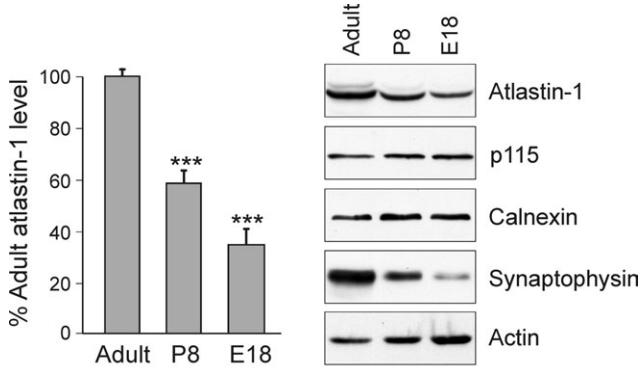

Figure 3. Atlastin-1 expression during rat brain development. (Right panel) Rat brain homogenates (20 μg protein/lane) from E18 to adult were immunoblotted with the indicated antibodies. Sizes of proteins after SDS–PAGE: atlastin-1, 64 kDa; p115, 115 kDa; calnexin, 90 kDa; synaptophysin, 38 kDa; actin, 42 kDa. (Left panel) Atlastin-1 levels were quantified and expressed as a percentage of the adult level. Results were plotted as mean ± SD of four independent experiments. $^{***}P < 0.001$. There were no significant changes in levels of calnexin and p115 from E18 to adult (data not shown).

very little AP-2 immunostaining detected within the Golgi apparatus (Fig. 6D).

Using electron microscopy, we probed further the subcellular localization of atlastin-1 in cultured neurons. As reported previously (9), we again observed immunogold particles decorating the Golgi apparatus (Fig. 7A) and, to a lesser degree, the ER (Fig. 7B). In addition, within axonal growth cones and varicosities, atlastin-1 labeling was prominent on vesicular structures, but it did not appear to be present on the plasma membrane (Fig. 7C). Along neuronal processes, a number of vesicular structures were labeled, but again plasma membrane labeling was not clearly evident (data not shown). There was no detectable staining at synapses in the cultured neurons

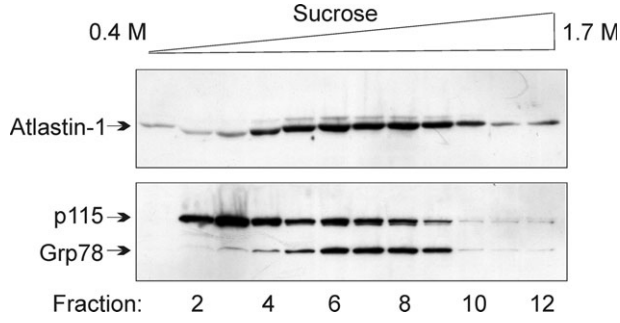

Figure 4. Sucrose density gradient fractionation of atlastin-1 in cultured cortical neurons. Homogenates prepared from cultured rat cortical neurons were subjected to sucrose gradient density centrifugation, and the 12 fractions collected were immunoblotted for atlastin-1 (64 kDa), p115 (115 kDa) and Grp78 (78 kDa; anti-KDEL antibodies). Fraction numbers are indicated along the bottom.

(Fig. 7D). Similarly, in immunoelectron microscopy studies evaluating sections from adult rat brain cerebral cortex, atlastin-1 staining was not detected at synapses, although there was clear labeling of the Golgi apparatus and, to a much lesser extent, the ER (Supplementary Material, Fig. S2A and B).

Atlastin-1 knock-down in neurons inhibits axon growth

Over-expression of epitope-tagged wild-type atlastin-1 and various SPG3A mutant forms of atlastin-1 resulted in extensive distribution throughout the ER network, in contrast to the predominant localization of the endogenous protein to the Golgi apparatus (data not shown). Thus, to model SPG3A in cultured cortical neurons, we knocked down expression of atlastin-1 using small hairpin RNAs (shRNAs). We utilized a vector, pG-SUPER, that expresses both the shRNA and GFP, which can be used to identify knock-down cells using fluorescent microscopy (18). With this technique, atlastin-1 protein in transfected neurons was nearly undetectable at 6 days *in vitro* (DIV6) (Fig. 8A), but levels of Golgi markers such as p115 did not change (Fig. 8B); atlastin-1 immunostaining was also markedly reduced within the axonal growth cones and varicosities (data not shown).

We next assessed the role of atlastin-1 in axonal development using these shRNA techniques (Fig. 9). In cultured cortical neurons in which atlastin-1 expression was suppressed, there was a much greater percentage of neurons lacking axons at DIV6 when compared with neurons transfected with the control pG-SUPER vector (Fig. 9A, B and D). In those cells with axons, the axons in the atlastin-1 shRNA expressing cells were significantly shorter when compared with those in control pG-SUPER-transfected cells (Fig. 9A, B and C). In particular, the number of neurons with long axons (>500 μm) was markedly reduced in the atlastin-1 shRNA (one out of 49) versus control (eight out of 43) transfections. Lastly, the number of primary dendrites was also modestly but consistently reduced in the shRNA-transfected neurons when compared with the controls (Fig. 9E).

Downloaded from https://academic.oup.com/hmg/article/15/8/1343/644573 by guest on 23 April 2024

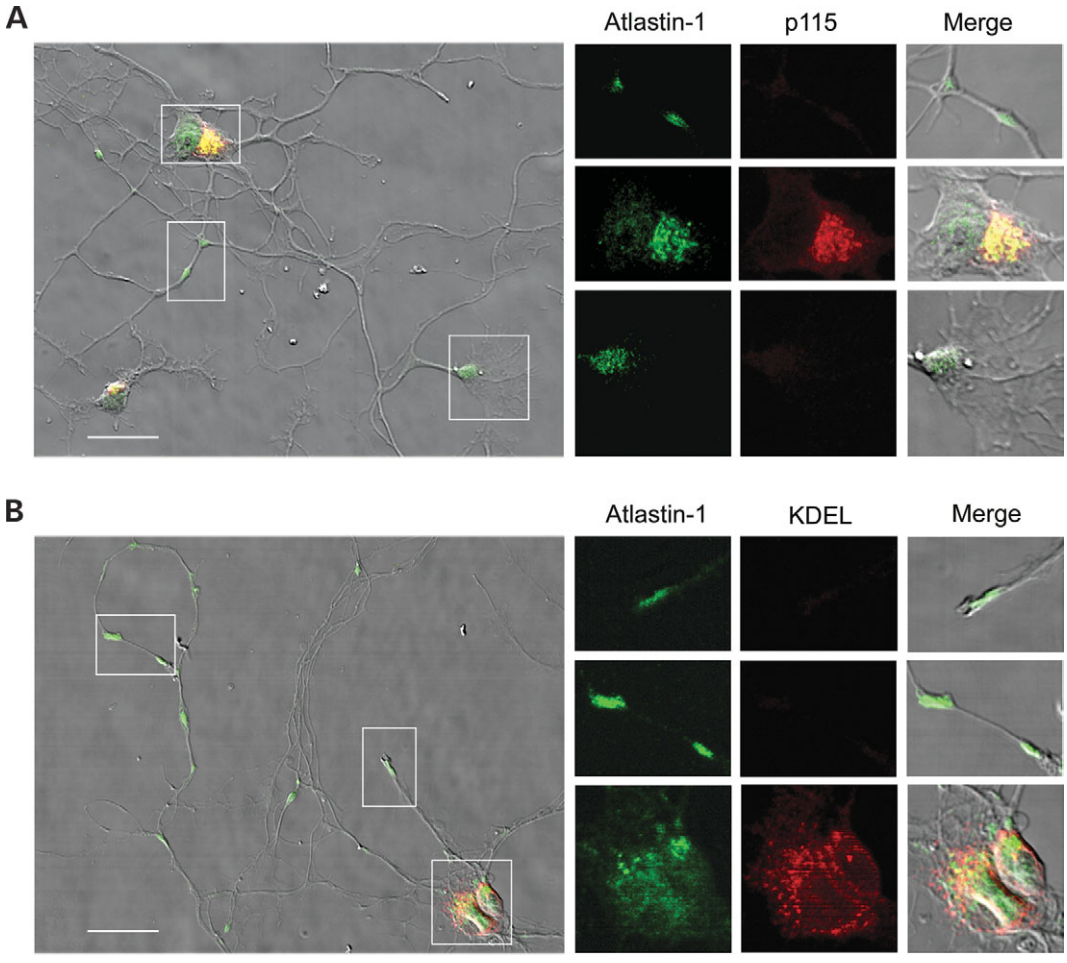

Figure 5. Enrichment of atlastin-1 in axonal growth cones and varicosities visualized by confocal immunofluorescence microscopy. (**A**) Cultured cortical neurons were co-stained with antibodies against atlastin-1 and the Golgi marker p115 and imaged using fluorescence microscopy. Boxed areas in the phase contrast superimposed image on the left are enlarged on the right. There is co-localization of atlastin-1 with p115 in the cell soma (right middle panels), but atlastin-1 alone is present in axonal varicosities, branch sites (right upper panels) and growth cones (right lower panels). (**B**) Cultured neurons were co-stained with antibodies against atlastin-1 and the ER marker KDEL, and the images are presented as earlier. There is partial co-localization of atlastin-1 with KDEL (right lower panels) in the soma, but there is no KDEL staining in the atlastin-1 enriched axonal varicosities (right middle panels) and growth cones (right upper panels). Scale bars, 20 μm.

DISCUSSION

In this study, we have demonstrated that several SPG3A mutant forms of atlastin-1 have impaired GTPase activity while retaining the ability to form oligomeric complexes. We propose that a net loss of overall GTPase activity of the atlastin-1 oligomer is likely due to the fact that SPG3A mutant atlastin-1 proteins can form mixed homo-oligomers with the wild-type protein in a dominant-negative fashion. Such a mechanism is highly reminiscent of that suggested for neurological disorders due to mutations in other members of the dynamin superfamily such as OPA1 (optic atrophy type 1) (19), dynamin 2 (intermediate Charcot–Marie–Tooth neuropathy) (20) and Mfn2 (Charcot–Marie–Tooth neuropathy type 2A) (21–24), which have roles in vesicle formation or organelle fission and fusion (8). Indeed, all of these proteins are oligomers, and in all cases, the inheritance of the disorders is autosomal dominant. Interestingly, for many of these disorders, including SPG3A (Supplementary Material, Fig. S1) (7), a large number of missense mutations have been identified, often distributed throughout the protein and not necessarily limited to any particular functional domain. This sensitivity of different dynamin-like GTPases to apparently subtle changes in protein structure may reflect the complex structural rearrangements required of proteins in this family (25). Of course, some mutations may not impact GTPase activity directly, but instead may result in impaired protein function through an increased susceptibility to protein degradation, changes in oligmerization or altered interactions with other proteins.

Many studies have noted that SPG3A is among the most early-onset forms of HSP and that it is also slowly progressive or even non-progressive in some cases, giving rise to suggestions that it may be a developmental disorder (2,7,11–15). Furthermore, a recent MRI study noted that patients with SPG3A had less severe atrophy in spite of worse clinical features than patients with other pure HSPs such as SPG6 and

Downloaded from https://academic.oup.com/hmg/article/15/8/1343/644573 by guest on 23 April 2024

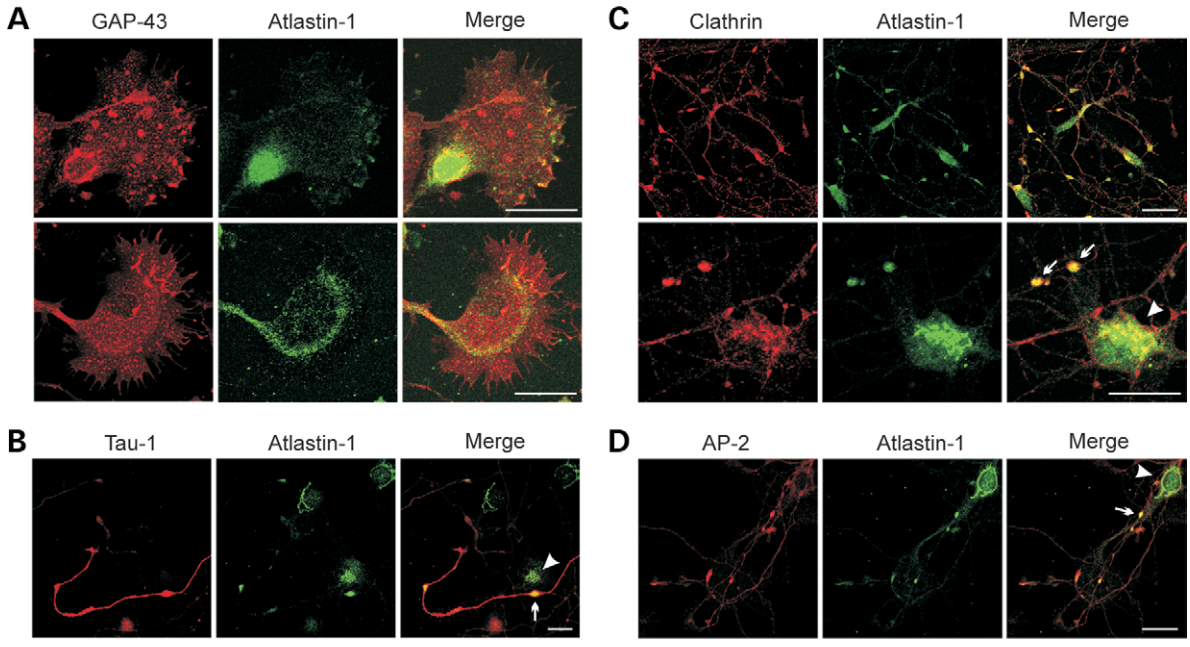

Figure 6. Co-localization of atlastin-1 with other proteins in axonal growth cones and varicosities. Cultured rat cortical neurons were co-stained with antibodies against atlastin-1 and the indicated marker proteins and imaged using confocal microscopy. (**A**) Atlastin-1 shows limited co-localization with GAP-43 in growth cones. Although atlastin-1 is often highly enriched in the C-domain (upper panels), in some cases, it localizes instead to the P-domain (lower panels). (**B**) Co-localization of atlastin-1 and the axon marker tau-1 in axonal varicosities (arrow). Tau-1 is not present in the Golgi apparatus (arrowhead). (**C**) In varicosities along axons, atlastin-1 co-localizes closely with clathrin (arrows in higher magnification lower panel). More limited co-localization is also seen in the Golgi apparatus (arrowhead). (**D**) Co-localization of AP-2 with atlastin-1 in axonal varicosities (arrow), but AP-2 is not enriched in the Golgi apparatus (arrowhead). Scale bars, 20 μm.

SPG8, again supporting alternative mechanisms that do not rely solely on axonal degeneration (26). Our findings of atlastin-1 localization within growth cones and the effects of its loss on axonal growth provide important insights into the function of atlastin-1 during development and are highly consistent with many published clinical studies, particularly those emphasizing the early onset and often lack of apparent progression of SPG3A (2).

Although atlastin-1 is critical for the formation and elongation of axons during development, the molecular mechanisms involved remain unclear. On the basis of its localization in the neuronal soma, atlastin-1 seems likely to be involved in ER–Golgi membrane trafficking, perhaps in membrane fusion events based on its topological similarities to two other dynamin superfamily members, the mitofusins Mfn1 and Mfn2 (27), which mediate mitochondrial fusion. However, the localization of atlastin-1 within growth cones diverges markedly from those of markers of both the ER and the Golgi apparatus, indicating that atlastin-1 also has functions in another membrane compartment during axonal development. A particularly intriguing finding of our study is that atlastin-1 appears to have two strikingly different localizations within growth cones. In some cases, it is condensed within the C-domain, and in others, it is present more peripherally in the P-domain (Fig. 6A). The most likely explanation for these differences is that atlastin-1 undergoes dynamic changes in localization that are related to the growth or pathfinding of the axon during development. As the arrival of an axonal varicosity, or 'wave', at a growth cone correlates closely with the onset of a growth phase (17), an attractive molecular mechanism for atlastin-1 function in axonal elongation would be the regulation of membrane dynamics within the growth cone, because membrane expansion, in concert with cytoskeletal dynamics, is an important mediator of axon elongation (28–31). Live imaging studies should help to uncover how changes in the axonal localization of atlastin-1 correlate with the dynamic changes occurring in growth cones during axonal development.

Interestingly, a recent study has identified an interaction of atlastin-1 with spastin (32), a microtubule-severing ATPase that is mutated in the most common form of autosomal dominant HSP, SPG4 (33–36), indicating that these HSP proteins may be involved in a common cellular pathway (32). In fact, spastin is also enriched in the growth cones and branch points of neurites in the NSC34 neuron-like cell line (37), highly reminiscent of the localization of atlastin-1 that we report here in cultured neurons. As destabilized microtubules are commonly found in growth cones and at axonal branch points (38), it will be important to determine whether the microtubule-severing protein spastin is co-localized with atlastin-1 in these areas during neuronal development and whether they interact *in vivo*. If so, spastin may function with atlastin-1 in membrane trafficking events in addition to its known effects on microtubule dynamics.

In summary, we have shown that atlastin-1 mutations result in a net loss of function of the atlastin-1 GTPase and that impairment in atlastin-1 function in neurons gives rise to abnormalities of axonal development, which are likely highly relevant to the pathogenesis of SPG3A HSP, with its characteristic features of early onset along with slow

Downloaded from https://academic.oup.com/hmg/article/15/8/1343/644573 by guest on 23 April 2024

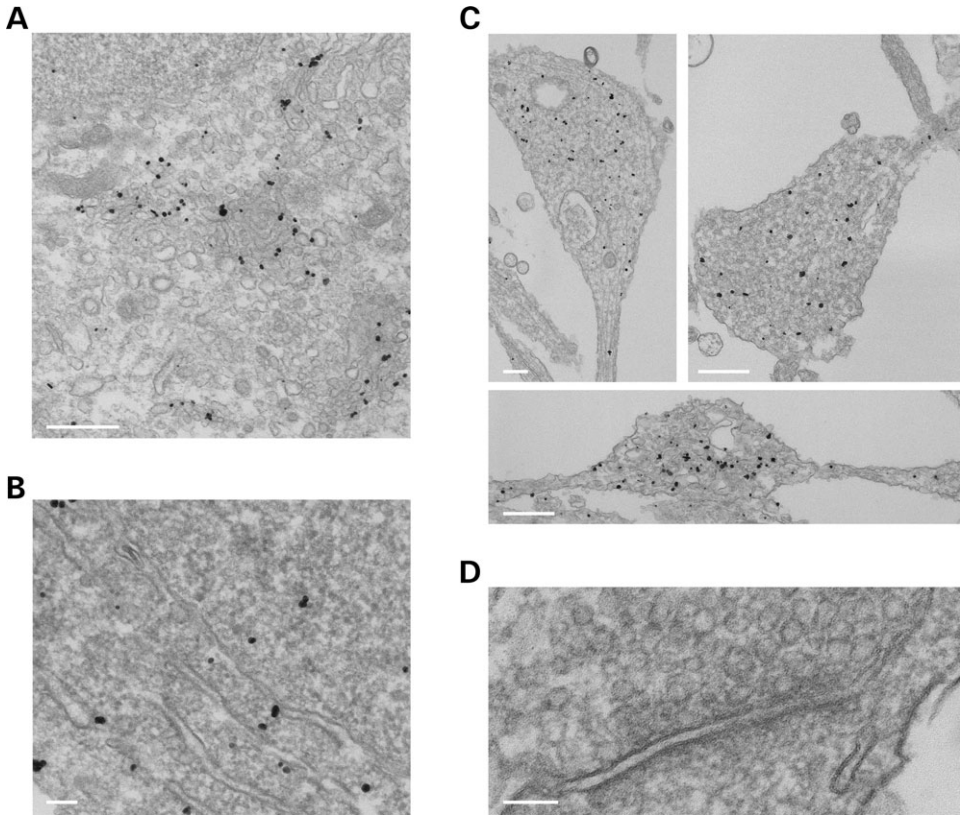

Figure 7. Atlastin-1 localization to vesicular structures within axonal growth cones and varicosities in cultured neurons by immunogold electron microscopy. Localization of atlastin-1 to the Golgi apparatus (**A**) and the ER (**B**). (**C**) Localization of atlastin-1 within growth cones (upper panels) and an axonal varicosity (lower panel). (**D**) Atlastin-1 is not present at synapses. Scale bars: (A and C) 500 nm; (B and D) 100 nm.

progression or even lack of progression. Studies examining the effects of atlastin-1 on membrane expansion at the growth cone as well as in ER–Golgi trafficking will be necessary to further understand the diverse functional roles of atlastin-1 within neurons.

MATERIALS AND METHODS

DNA constructs

pGAD10-, pBHA- and pCAL-n-EK-atlastin-1 yeast two-hybrid and bacterial fusion protein constructs as well HA- and Myc-tagged atlastin-1 eukaryotic expression constructs have been described previously (9). The Myc-tagged Drp1 construct was also described previously (39). Site-directed mutagenesis was performed using the QuikChange method (Stratagene) and confirmed in each construct by DNA sequencing.

An oligoduplex shRNA based on nucleotides 1138–1156 of rat atlastin-1 (GenBank accession no. AY581896) was created by annealing the following primers: 5′-gatcccc CCGAGAGCC TAGATATTAAttcaagagaTTAATATCTAGGCTCTCGGttttt-3′ and 5′-agctaaaaaCCGAGAGCCTAGATATTAAtctcttgaa TTAATATCTAGGCTCTCGGggg-3′. This oligoduplex DNA was then directionally cloned into the *Bgl*II and *Hin*dIII restriction sites of the pG-SUPER vector (18).

Atlastin-1 interaction studies

Yeast two-hybrid tests were performed using the L40 yeast strain, harboring the reporter genes *HIS3* and β-*galactosidase* under the control of upstream LexA binding sites as described previously (9,39,40). Co-IP studies, membrane fractionation and FPLC gel-exclusion chromatography were performed as described in Zhu *et al*. (9,39). For chemical cross-linking studies, COS-7 cells over-expressing wild-type atlastin-1 or SPG3A mutants were washed twice with phosphate-buffered saline (PBS) and lysed; the post-nuclear supernatant was then incubated with 0.7 mM BS^3 (Pierce) in PBS for 2 h on ice. After the reactions were quenched with 1 M Tris–HCl buffer (pH 7.5), proteins were resolved by SDS–PAGE (6% acrylamide gels) and immunoblotted with anti-Myc antibodies as described previously (9).

Tissue preparation and cell fractionation

Brains from adult (150–200 g), post-natal day 8 (P8) and E18 Sprague–Dawley rats were homogenized in PBS with 0.5% Triton X-100 and protease inhibitor cocktail (Sigma-Aldrich). After centrifugation (20 min, 55 000*g*, 4°C), the supernatants were resolved on 10% SDS–PAGE gels and immunoblotted with antibodies against atlastin-1 (1.4 μg/ml) (9), p115 (mouse monoclonal clone 15, IgG_1; BD Biosciences Pharmingen; 1:2000), KDEL (mouse monoclonal 10C3,

Downloaded from https://academic.oup.com/hmg/article/15/8/1343/644573 by guest on 23 April 2024

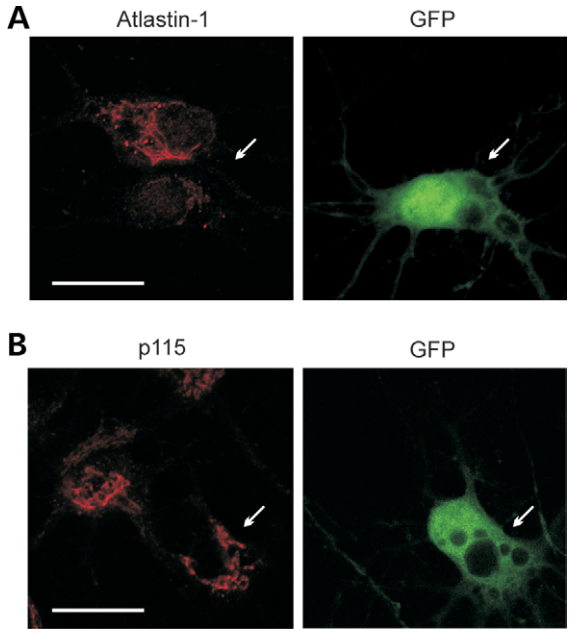

Figure 8. Knock-down of atlastin-1 expression in neurons by shRNA. (**A**) Atlastin-1 levels in pG-SUPER atlastin-1 shRNA-expressing cells (arrows), identified by GFP co-expression, are markedly reduced when compared with the neighboring untransfected cell. Neurons expressing the control pG-SUPER plasmid showed no changes in atlastin-1 expression (data not shown). (**B**) Levels of markers for the Golgi apparatus such as p115 are not changed in pG-SUPER atlastin-1 shRNA-expressing cells (arrows). Scale bars, 20 μm.

IgG_{2a}; Stressgen Biotech; 1:1500), actin (mouse monoclonal AC-40, IgG_{2a}; Sigma-Aldrich; 1:2000) or synaptophysin (rabbit polyclonal; Santa Cruz; 1:2000) as described previously (9). Immunoblots were scanned using a DuoScan T2500 scanner (Agfa), and protein levels were then quantitatively analyzed using ImageQuant5.1 (Molecular Dynamics).

Neurons in primary culture (DIV6) were collected in ice-cold buffer A [25 mM MES (pH 7.2) and 2 mM EDTA] with protease inhibitor cocktail, homogenized with a glass-Teflon homogenizer and centrifuged for (5 min, 1000*g*, 4°C). The supernatant was brought to a final concentration of 0.4 M sucrose before being overlaid onto a continuous 0.4–1.7 M sucrose gradient prepared in buffer A. After centrifugation in a Beckman SW50 rotor (12 h, 200 000*g*, 4°C), 12 fractions were collected. Samples were concentrated by methanol precipitation and resuspended in SDS–PAGE loading buffer, resolved by SDS–PAGE and immunoblotted with anti-KDEL, anti-atlastin-1 and anti-p115 antibodies as described earlier.

GTPase activity assays

Wild-type and SPG3A mutant CBP-atlastin-1 fusion proteins were prepared and purified, and the GTPase activity assays were performed using 0.2 μg protein/reaction as described previously (9,39). Data were compared using Student's *t*-test, and differences were considered to be significant if $P < 0.05$.

Neuronal cultures, transfections and immunocytochemistry

All animal experiments were approved by the NINDS/NIDCD Animal Care and Use Committee. Primary cultures of rat cerebral cortical neurons were prepared from E18 embryos, plated at a density of $\sim 2.6 \times 10^4/cm^2$ on cover slips and maintained as described previously (41). At DIV6, neurons were fixed with paraformaldehyde, immunostained with primary and Alexa Fluor 488 and 568 secondary antibodies (Molecular Probes), mounted and imaged using a Zeiss LSM510 laser-scanning confocal microscope as described previously (9). Primary antibodies against the following proteins were used: atlastin-1 (no. 5409; 7 μg/ml) (9); p115 (mouse monoclonal clone 15, IgG_1; BD Biosciences Pharmingen; 1:500 dilution); KDEL (mouse monoclonal 10C3, IgG_{2a}; Stressgen Biotech; 1:200 dilution); GAP-43 (mouse monoclonal clone GAP-7B10, IgG_{2a}; Sigma-Aldrich; 1:500 dilution); clathrin heavy chain (mouse monoclonal clone X22, IgG_1; Affinity BioReagents; 1:500 dilution); α-adaptin (AP-2; mouse monoclonal clone AP6, IgG_1; Affinity BioReagents; 1:500 dilution).

For shRNA-mediated knock-down of atlastin-1, rat cerebral cortical neurons were transfected with pG-SUPER or pG-SUPER atlastin-1 shRNA immediately after dissociation by electroporation (Amaxa Nucleofector I); cells were then plated at $\sim 1.3 \times 10^4/cm^2$ onto cover slips precoated with poly-L-lysine. At DIV6, neurons were fixed for 30 min with 4% formaldehyde and then blocked with 5% normal goat serum and 0.2% saponin in PBS for 30 min. Primary antibodies diluted in PBS with 5% normal goat serum and 0.05% saponin were incubated with the cover slips overnight at 4°C, and then Alexa Fluor secondary antibodies (Molecular Probes; 1:1000) diluted in the same medium were applied for 1 h at 25°C. Axons were stained with anti-tau-1 antibody (mouse monoclonal PC1C6, IgG_{2a}; Chemicon; 1:500 dilution), followed by Alexa Fluor 568 conjugated goat anti-mouse IgG_{2a} antibody. Dendrites were stained with antibody against MAP2 (mouse monoclonal HM-2, IgG_1; Sigma-Aldrich, 1:500 dilution), followed by Alexa Fluor 350 conjugated goat anti-mouse IgG_1 secondary antibodies. Atlastin-1 protein levels were monitored using rabbit polyclonal anti-atlastin-1 antibodies (9), followed by Alexa Fluor 633 conjugated goat anti-rabbit IgG secondary antibodies. Fluorescent images were acquired using a Zeiss LSM510 NLO laser-scanning confocal microscope with a Mira-Verdi laser system for multiphoton excitation. Alexa Fluor 488 was excited with $\lambda = 488$ nm illumination; Alexa Fluor 568 with $\lambda = 543$ nm; Alexa Fluor 633 with $\lambda = 633$ nm; Alexa Fluor 350 with $\lambda = 730$ nm (two photon excitation). Measurements of axon length were performed using ImageJ software (NIH), and statistical analyses were performed using Student's *t*-test and K^2-test.

Immunogold electron microscopy

Rat hippocampal and cerebral cortical neuron cultures were prepared and maintained as described previously (41,42). After 3–4 weeks (for hippocampal neurons) or 6 days (for cortical neurons) in culture, the neurons were fixed with 4%

Downloaded from https://academic.oup.com/hmg/article/15/8/1343/644573 by guest on 23 April 2024

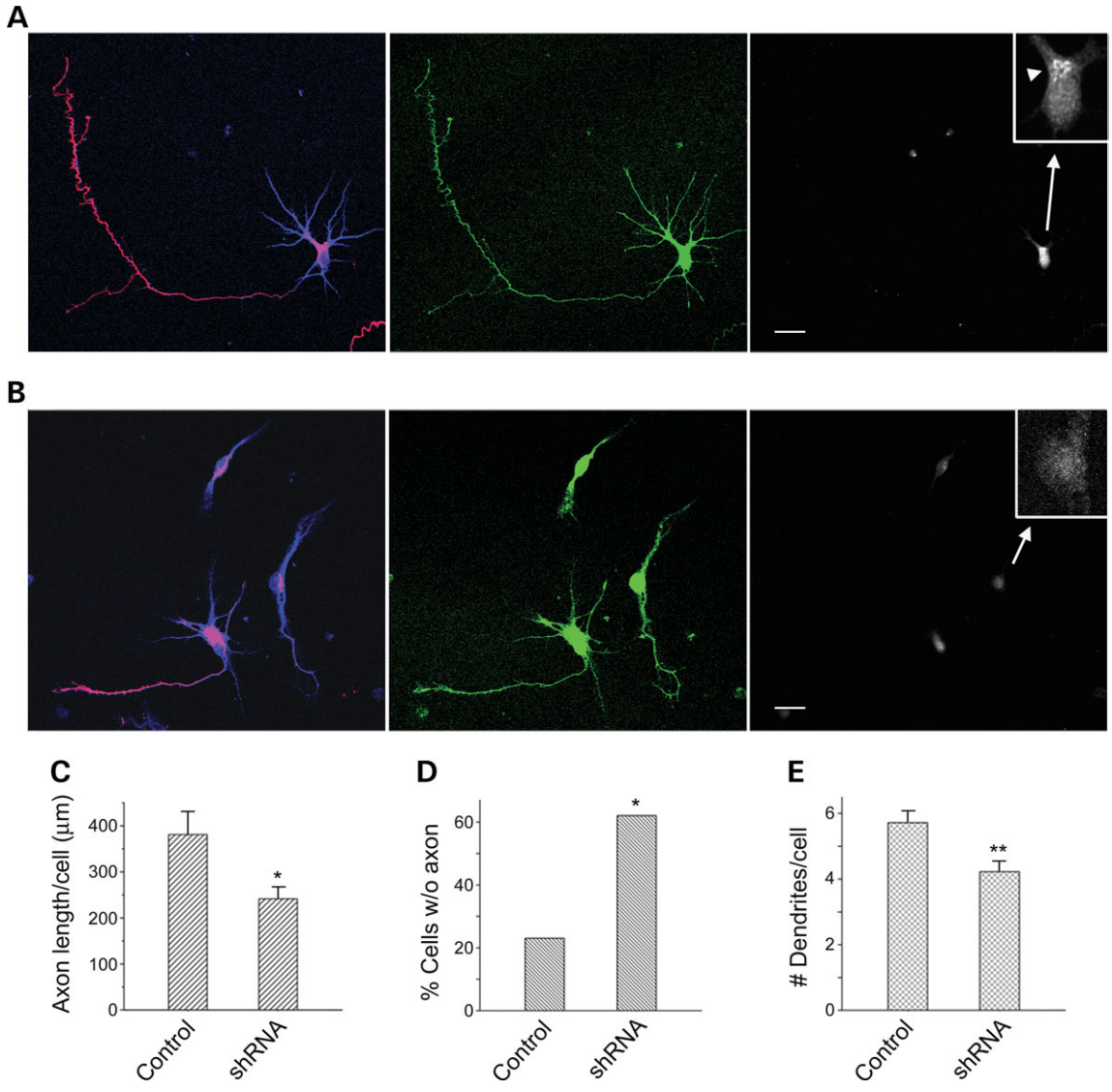

Figure 9. Knock-down of atlastin-1 expression inhibits axon formation and elongation in cultured cortical neurons. (**A** and **B**) Left images are double labeled for axons (tau-1; red) and dendrites (MAP2; blue), and middle images identify pG-SUPER-transfected cells using GFP detection (green). Right images show atlastin-1 immunoreactivity (white; enlarged in insets). Atlastin-1 staining in Golgi apparatus of a control pG-SUPER-transfected cell is indicated by an arrowhead in the inset of (A), but no Golgi staining is visualized in the shRNA-expressing cells shown in (B) (see inset), confirming knock-down of expression. Background fluorescence is accentuated in the right panels to facilitate cell identification. (A) Neurons transfected with control pG-SUPER vector exhibited no changes in axonal or dendritic appearance when compared with untransfected cells at DIV6. (B) In cells expressing the pG-SUPER atlastin-1 shRNA, many cells have shortened axons (bottom cell) or else lack axons entirely (middle and upper cells). The effects of atlastin-1 shRNA knock-down on axon length (**C**), the percentage of cells lacking axons (**D**) and the number of dendrites per cell (**E**) are shown graphically ($n = 43$ for control pG-SUPER; $n = 49$ for shRNA). In (C and E), results are mean $\pm$ SD. $^{*}P < 0.05$; $^{**}P < 0.01$. Scale bars, 20 μm.

paraformaldehyde or else 2% paraformaldehyde and 0.1% glutaraldehyde in 0.1 M phosphate buffer (pH 7.4) for 30 min. After washing with 0.1 M phosphate buffer, cells were permeabilized and blocked with 5% normal goat serum and 0.1% saponin in PBS for 1 h. Rabbit polyclonal anti-atlastin-1 (no. 5409; 14 μg/ml) or anti-synaptophysin (DAKA; 1:250 dilution) antibodies were then added in blocking buffer for 1 h; in control experiments, the primary antibody was omitted. After washing with 1% normal goat serum in PBS and 2% non-fat milk in PBS, cells were incubated with 1.4 nm Nanogold gold-conjugated anti-rabbit secondary antibodies (1:250 dilution; Nanoprobes) in 2% non-fat milk in PBS for 1 h. After washing with 2% non-fat milk in PBS, cells were then fixed with 2% glutaraldehyde in PBS for 30 min. Cells were thoroughly washed with PBS and distilled water, silver-enhanced using the HQ silver kit (Nanoprobes) and washed again with water and 0.1 M phosphate buffer. The fixed cells were then treated with 0.2% OsO_4 in 0.1 M phosphate buffer for 30 min, mordanted *en bloc* with 0.25% uranyl acetate in acetate buffer (pH 5.0) overnight, washed and dehydrated with serial concentrations of ethanol and finally infiltrated and embedded in epoxy resins.

Downloaded from https://academic.oup.com/hmg/article/15/8/1343/644573 by guest on 23 April 2024

Thin sections of ~70 nm were counterstained with uranyl acetate and lead citrate and examined under a Jeol 1200 EXII transmission electron microscope. Digital images were acquired using an XR-100 CCD camera (Advanced Microscopy Techniques) and processed with Adobe Photoshop software.

For immunogold labeling of adult rat brain sections, adult Sprague–Dawley rats (150–200 g) were perfused with 4% paraformaldehyde and 100 μm sections were prepared. Immunogold staining and electron microscopy were then performed as described previously for the cultured neurons.

Protein content determination

Protein concentrations were assayed using the bicinchoninic acid assay kit (Pierce), with bovine serum albumin as the standard.

SUPPLEMENTARY MATERIAL

Supplementary Material is available at HMG Online.

ACKNOWLEDGEMENTS

We thank Drs G. Borisy and S. Kojima for providing the pG-SUPER plasmid, Dr C.L. Smith (NINDS Light Imaging Facility) for assistance with confocal microscopy, C. Winters for providing mature rat hippocampal neuron cultures and J. Nagle and D. Kaufmann (NINDS DNA Sequencing Facility) for DNA sequencing. This work was supported by the Intramural Research Program of the National Institute of Neurological Disorders and Stroke, National Institutes of Health.

Conflict of Interest statement. None declared.

REFERENCES

1. Crosby, A.H. and Proukakis, C. (2002) Is the transportation highway the right road for hereditary spastic paraplegia? *Am. J. Hum. Genet.*, **71**, 1009–1016.
2. Fink, J.K. (2003) Advances in the hereditary spastic paraplegias. *Exp. Neurol.*, **184**, S106–S110.
3. Reid, E. (2003) Science in motion: common molecular pathological themes emerge in the hereditary spastic paraplegias. *J. Med. Genet.*, **40**, 81–86.
4. Soderblom, C. and Blackstone, C. (2006) Traffic accidents: molecular genetic insights into the pathogenesis of the hereditary spastic paraplegias. *Pharmacol. Ther.*, **109**, 42–56.
5. Harding, A.E. (1983) Classification of the hereditary ataxias and paraplegias. *Lancet*, **1**, 1151–1155.
6. Zhao, X., Alvarado, D., Rainier, S., Lemons, R., Hedera, P., Weber, C.H., Tukel, T., Apak, M., Heiman-Patterson, T., Ming, L. *et al*. (2001) Mutations in a newly identified GTPase gene cause autosomal dominant hereditary spastic paraplegia. *Nat. Genet.*, **29**, 326–331.
7. Namekawa, M., Ribai, P., Nelson, I., Forlani, S., Fellmann, F., Goizet, C., Depienne, C., Stevanin, G., Ruberg, M., Dürr, A. and Brice, A. (2006) SPG3A is the most frequent cause of hereditary spastic paraplegia with onset before age 10 years. *Neurology*, **66**, 112–114.
8. Praefcke, G.J.K. and McMahon, H.T. (2004) The dynamin superfamily: universal membrane tubulation and fission molecules? *Nat. Rev. Mol. Cell Biol.*, **5**, 133–147.
9. Zhu, P.-P., Patterson, A., Lavoie, B., Stadler, J., Shoeb, M., Patel, R. and Blackstone, C. (2003) Cellular localization, oligomerization, and membrane association of the hereditary spastic paraplegia 3A (SPG3A) protein atlastin. *J. Biol. Chem.*, **278**, 49063–49071.
10. Muglia, M., Magariello, A., Nicoletti, G., Patitucci, A., Gabriele, A.L., Conforti, F.L., Mazzei, R., Caracciolo, M., Ardito, B., Lastilla, M. *et al*. (2002) Further evidence that *SPG3A* gene mutations cause autosomal dominant hereditary spastic paraplegia. *Ann. Neurol.*, **51**, 794–795.
11. Dalpozzo, F., Rossetto, M.G., Boaretto, F., Sartori, E., Mostacciuolo, M.L., Daga, A., Bassi, M.T. and Martinuzzi, A. (2003) Infancy onset hereditary spastic paraplegia associated with a novel atlastin mutation. *Neurology*, **61**, 580–581.
12. Wilkinson, P.A., Hart, P.E., Patel, H., Warner, T.T. and Crosby, A.H. (2003) SPG3A mutation screening in English families with early onset autosomal dominant hereditary spastic paraplegia. *J. Neurol. Sci.*, **216**, 43–45.
13. Abel, A., Fonknechten, N., Hofer, A., Dürr, A., Cruaud, C., Voit, T., Weissenbach, J., Brice, A., Klimpe, S., Auburger, G. and Hazan, J. (2004) Early onset autosomal dominant spastic paraplegia caused by novel mutations in SPG3A. *Neurogenetics*, **5**, 239–243.
14. Dürr, A., Camuzat, A., Colin, E., Tallaksen, C., Hannequin, D., Coutinho, P., Fontaine, B., Rossi, A., Gil, R., Rousselle, C. *et al*. (2004) Atlastin1 mutations are frequent in young-onset autosomal dominant spastic paraplegia. *Arch. Neurol.*, **61**, 1867–1872.
15. Hedera, P., Fenichel, G.M., Blair, M. and Haines, J.L. (2004) Novel mutation in the *SPG3A* gene in an African American family with an early onset of hereditary spastic paraplegia. *Arch. Neurol.*, **61**, 1600–1603.
16. Ruthel, G. and Banker, G. (1998) Actin-dependent anterograde movement of growth-cone-like structures along growing hippocampal axons: a novel form of axonal transport? *Cell Motil. Cytoskeleton*, **40**, 160–173.
17. Ruthel, G. and Banker, G. (1999) Role of moving growth cone-like 'wave' structures in the outgrowth of cultured hippocampal axons and dendrites. *J. Neurobiol.*, **39,** 97–106.
18. Kojima, S., Vignjevic, D. and Borisy, G.G. (2004) Improved silencing vector co-expressing GFP and small hairpin RNA. *BioTechniques*, **36**, 74–79.
19. Delettre, C., Lenaers, G., Pelloquin, L., Belenguer, P. and Hamel, C.P. (2002) OPA1 (Kjer type) dominant optic atrophy: a novel mitochondrial disease. *Mol. Genet. Metab.*, **75**, 97–107.
20. Züchner, S., Noureddine, M., Kennerson, M., Verhoeven, K., Claeys, K., De Jonghe, P., Merory, J., Oliveira, S.A., Speer, M.C., Stenger, J.E. *et al*. (2005) Mutations in the pleckstrin homology domain of dynamin 2 cause dominant intermediate Charcot–Marie–Tooth disease. *Nat. Genet.*, **37**, 289–294.
21. Züchner, S., Mersiyanova, I.V., Muglia, M., Bissar-Tadmouri, N., Rochelle, J., Dadali, E.L., Zappia, M., Nelis, E., Patitucci, A., Senderek, J. *et al*. (2004) Mutations in the mitochondrial GTPase mitofusin 2 cause Charcot–Marie–Tooth neuropathy type 2A. *Nat. Genet.*, **36**, 449–451.
22. Kijima, K., Numakura, C., Izumino, H., Umetsu, K., Nezu, A., Shiiki, T., Ogawa, M., Ishizaki, Y., Kitamura, T., Shozawa, Y. and Hayasaka, K. (2005) Mitochondrial GTPase mitofusin 2 mutation in Charcot–Marie–Tooth neuropathy type 2A. *Hum. Genet.*, **116**, 23–27.
23. Lawson, V.H., Graham, B.V. and Flanigan, K.M. (2005) Clinical and electrophysiologic features of CMT2A with mutations in the mitofusin 2 gene. *Neurology*, **65**, 197–204.
24. Zhu, D., Kennerson, M.L., Walizada, G., Züchner, S., Vance, J.M. and Nicholson, G.A. (2005) Charcot–Marie–Tooth with pyramidal signs is genetically heterogeneous: families with and without *MFN2* mutations. *Neurology*, **65**, 496–497.
25. Zhang, P. and Hinshaw, J.E. (2001) Three-dimensional reconstruction of dynamin in the constricted state. *Nat. Cell Biol.*, **3**, 922–926.
26. Hedera, P., Eldevik, O.P., Maly, P., Rainier, S. and Fink, J.K. (2005) Spinal cord magnetic resonance imaging in autosomal dominant hereditary spastic paraplegia. *Neuroradiology*, **47**, 730–734.
27. Chen, H. and Chan, D.C. (2005) Emerging functions of mammalian mitochondrial fusion and fission. *Hum. Mol. Genet.*, **14**(Suppl. 2), R283–R289.
28. Baas, P.W. and Luo, L. (2001) Signaling at the growth cone: the scientific progeny of Cajal meet in Madrid. *Neuron*, **32**, 981–984.
29. Goldberg, J.L. (2003) How does an axon grow? *Genes Dev.*, **17**, 941–958.
30. Goldberg, J.L. (2004) Intrinsic neuronal regulation of axon and dendrite growth. *Curr. Opin. Neurobiol.*, **14**, 551–557.

Downloaded from https://academic.oup.com/hmg/article/15/8/1343/644573 by guest on 23 April 2024

31. Pfenninger, K.H., Laurino, L., Peretti, D., Wang, X., Rosso, S., Morfini, G., Cáceres, A. and Quiroga, S. (2003) Regulation of membrane expansion at the nerve growth cone. *J. Cell Sci.*, **116**, 1209–1217.
32. Sanderson, C.M., Connell, J.W., Edwards, T.L., Bright, N.A., Duley, S., Thompson, A., Luzio, J.P. and Reid, E. (2006) Spastin and atlastin, two proteins mutated in autosomal-dominant hereditary spastic paraplegia, are binding partners. *Hum. Mol. Genet.*, **15**, 307–318.
33. Evans, K.J., Gomes, E.R., Reisenweber, S.M., Gundersen, G.G. and Lauring, B.P. (2005) Linking axonal degeneration to microtubule remodeling by spastin-mediated microtubule severing. *J. Cell Biol.*, **168**, 599–606.
34. Roll-Mecak, A. and Vale, R.D. (2005) The *Drosophila* homologue of the hereditary spastic paraplegia protein, spastin, severs and dissociates microtubules. *Curr. Biol.*, **15**, 650–655.
35. Trotta, N., Orso, G., Rossetto, M.G., Daga, A. and Broadie, K. (2004) The hereditary spastic paraplegia gene, *spastin*, regulates microtubule stability to modulate synaptic structure and function. *Curr. Biol.*, **14**, 1135–1147.
36. Sherwood, N.T., Sun, Q., Xue, M., Zhang, B. and Zinn, K. (2004) *Drosophila* spastin regulates synaptic microtubule networks and is required for normal motor function. *PLoS Biol.*, **2**, e429.
37. Errico, A., Claudiani, P., D'Addio, M. and Rugarli, E.I. (2004) Spastin interacts with the centrosomal protein NA14, and is enriched in the spindle pole, the midbody and the distal axon. *Hum. Mol. Genet.*, **13**, 2121–2132.
38. Kornack, D.R. and Giger, R.J. (2005) Probing microtubule +TIPs: regulation of axon branching. *Curr. Opin. Neurobiol.*, **15**, 58–66.
39. Zhu, P.-P., Patterson, A., Stadler, J., Seeburg, D.P., Sheng, M. and Blackstone, C. (2004) Intra- and intermolecular domain interactions of the C-terminal GTPase effector domain of the multimeric dynamin-like GTPase Drp1. *J. Biol. Chem.*, **279**, 35967–35974.
40. Blackstone, C., Roberts, R.G., Seeburg, D.P. and Sheng, M. (2003) Interaction of the deafness–dystonia protein DDP/TIMM8a with the signal transduction adaptor molecule STAM1. *Biochem. Biophys. Res. Commun.*, **305**, 345–352.
41. Zheng, Y.-l., Li, B.-S., Veeranna and Pant, H.C. (2003) Phosphorylation of the head domain of neurofilament protein (NF-M). *J. Biol. Chem.*, **278**, 24026–24032.
42. Lu, Z., McLaren, R.S., Winters, C.A. and Ralston, E. (1998) Ribosome association contributes to restricting mRNAs to the cell body of hippocampal neurons. *Mol. Cell. Neurosci.*, **12**, 363–375.

Downloaded from https://academic.oup.com/hmg/article/15/8/1343/644573 by guest on 23 April 2024